

EFFECTS OF THE DIFFERENT PRECIPITATION LEVELS ON SAR DATA

A.P.S.G.D.Toro^{a,1}, G. Capucci^{a,2}, J.P.S. Werner^{a,3}, I.T. Bueno^{b,4}, J.C.D.M. Esquerdo^{a,b,5}, J.F.G. Antunes^{b,6}, A.C.Coutinho^{b,7}, R.A.C. Lamparelli^{c,8}, P.S.G. Magalhães^c, J. G. Oliveira Júnior^{a,9}, G.K.D.A. Figueiredo^{a,10}

^a School of Agricultural Engineering - FEAGRI, University of Campinas - UNICAMP, 13083-875 Campinas, SP, Brazil

^b Embrapa Digital Agriculture, Brazilian Agricultural Research Corporation - EMBRAPA, 13083-886, Campinas, SP, Brazil

^c Interdisciplinary Center of Energy Planning - NIPE, University of Campinas, SP, Brazil

¹a265622@dac.unicamp.br, ²g167803@dac.unicamp.br, ³j164880@dac.unicamp.br, ⁴ibueno@unicamp.br, ⁵julio.esquerdo@embrapa.br,

⁶joao.antunes@embrapa.br, ⁷alex.coutinho@embrapa.br, ⁸lamparelli@unicamp.br, ⁹j164880@dac.unicamp.br, ¹⁰gleyce@unicamp.br

ABSTRACT

Agricultural monitoring systems based on optical satellite imagery aim to provide up-to-date information regarding large scale food production. However, the frequent presence of clouds during the annual crop cycle in tropical regions hampers image acquisition and leads to the use of images from active sensors (Radar), which are less affected by meteorological conditions such as precipitation. The present work aimed to identify the impacts of precipitation on the backscattering coefficient from Sentinel-1, in areas with agricultural landscape. We found no correlation between the precipitation and backscattering. In terms of classification accuracy, looks more advantageous to keep all crop images, given the greater accuracy and the shorter time in the processing.

Key words – SAR, Precipitation, Classification, NDVI.

1. INTRODUCTION

In the current population growth scenario, an increase of 70% in food production will be needed by 2050 compared to 2005 [1]. To achieve this goal, it is necessary to improve agricultural monitoring systems for better land use management and sustainable food production. Remote sensing techniques play a pivotal role in agricultural monitoring systems due to their ability to cover large areas [2]. However, most of these assessments are carried out with optical sensors, which are limited to the presence of clouds in tropical regions [3]. For this reason, the use of synthetic aperture radar (SAR) data has been exploited, since they are less affected by cloud interference [4], [5].

Despite the growing interest in using SAR data for agriculture, some factors directly affect its properties, such as the dielectric constant, which is related to humidity and precipitation [6]. Nevertheless, there is no consensus about how precipitation interferes with the backscattering coefficient.

Thus, this work aims to evaluate the use of SAR data for agricultural monitoring during periods of precipitation. From the results obtained it will be possible to infer the impact of precipitation on the backscattering coefficient in different crops and phenological stages.

2. MATERIAL AND METHODS

2.1. Study area

The study area is located in Sinop - Mato Grosso state (Figure 1). The region has climate type Am according to the Köppen classification, with short dry season [7]. The average annual precipitation ranges from 1800 to 2300 mm (Figure 2). The landscape of the region is composed of forest, pasture, and crops.

At the end of the crop year from 2020 to 2021, land use and land cover information were collected through field campaigns (Figure 1).

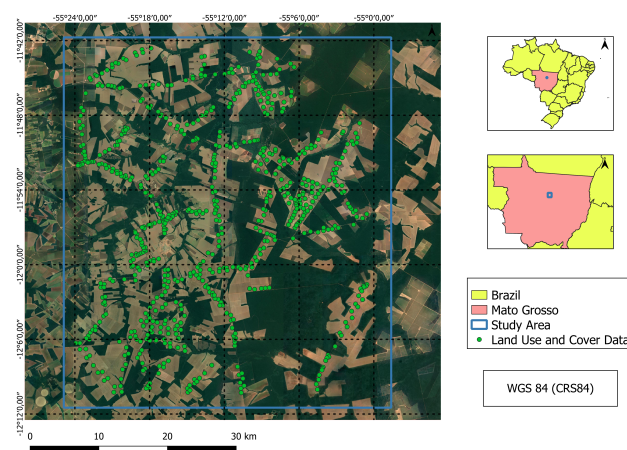


Figure 1: Study Area in Sinop region, Mato Grosso, Brazil.

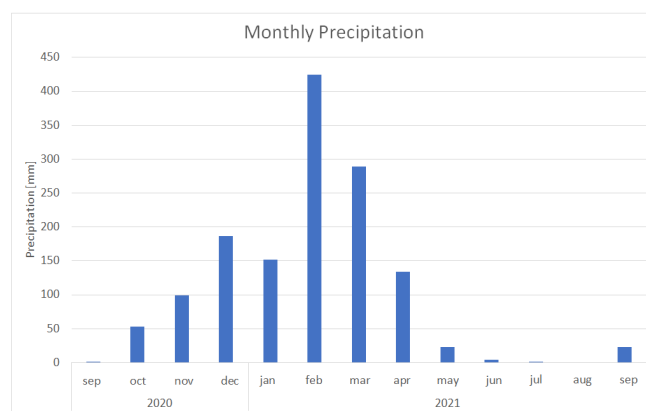


Figure 2: Monthly accumulated precipitation in the Sinop region, Mato Grosso, Brazil. Source: NASA POWER

2.2. Precipitation Data

The precipitation data were obtained from the MERRA-2 Satellite provided by the Prediction Of Worldwide Energy Resources (NASA POWER) platform. This product has a spatial resolution of 200 meters and precipitation information of millimeters per day. We acquired daily precipitation from September 2020 to August 2021 (one agricultural year), for the study area.

2.3. SAR data

We acquired SAR images from Sentinel 1 (A/B) satellites, which use a C band, with a frequency of 5.495 GHz, spatial resolution of 10 meters, and temporal resolution of 12 days (ESA, 2021). We acquired the acquisition mode Interferometric Wide (IW), which provides double polarization (vertical-vertical - VV and vertical-horizontal - VH). The other features of the images are processing Level 1, Single look complex (SLC), and Ground Range Detect (GRD). A total of 23 images were downloaded.

In addition, the preprocessing step was performed in the Sentinel Application Platform (SNAP) software. The preprocessing consisted of calibrating the images to obtain the backscatter coefficients, conversion of backscatter to decibels (Db), noise reduction using the Lee filter, and a terrain correction to correct geometric distortions [8] [9].

In addition to the VV and VH backscatter coefficients, coherence products were also acquired through Interferometry techniques (InSAR). InSAR is a technique that explores the phase difference between two SAR images, acquired under the same geometric conditions [10]. The similarity between both images works as a measure of the stability of the targets, and, therefore, has been applied in several studies aimed at agricultural monitoring [11]. Thus, from the Alaska Satellite Facility platform, 31 coherence products were obtained for the study area [12].

2.4. Optical data

To compare the phenological stage of the crop, precipitation levels, and their impacts on the backscatter coefficients, NDVI (Normalized Difference Vegetation Index) [13] images of Sentinel-2 satellite were acquired using Google Earth Engine (GEE) [14] platform. In total, 180 images were acquired for the agricultural year 2020/2021.

$$NDVI = \frac{NIR - RED}{NIR + RED} \quad (1)$$

Where NIR is the near infrared band and RED the red band.

The VV, VH, coherence, and NDVI data were normalized on a scale from 0 to 1 as shown in 3, 4 and 5. In addition, to evaluate the practical implications of removing or keeping products with precipitation occurrence, using Google Earth Engine [15], a supervised classification was executed. Two different scenarios were tested, the first using all the products

in one season of agricultural year (Sep - Aug), and the second only the products without precipitation in the 24 hours before image collection.

The classifier Support Vector Machine (SVM) [16] was used to classify the images into three different classes: native vegetation, pasture, and double crop. Confusion matrices were also generated for both scenarios and a table with accuracy for each scenario and the kappa index.

Due to the lack of representative classes by crop (number of samples greater than 30), it was decided to group the NDVI values of all crops to evaluate the impact of precipitation on the backscatter coefficient and coherence according to NDVI values. Then, the normalized NDVI values were subtracted from the mean and median values of the VV and VH and coherence signals (Table 1). Regarding precipitation, values were also grouped (considering the day of the satellite pass and the previous day) into classes, to compare whether the difference between NDVI and SAR values were altered according to the variation of precipitation values.

3. RESULTS

The behavior of the attributes analyzed mainly about crop development and precipitation, both backscatter values increase with the development of the crop and then decrease (Figure 3, 4 and 5). The behavior of coherence is the opposite, before the development of the crop it presents values closer to 1, indicating less change in the profile of the soil cover, and from the development of the crop, the value of coherence decreases, the alteration of the phenological stage of the plant causes this reduction, until at the end of the crop cycle the coherence value increases again and reaches values close to 1.

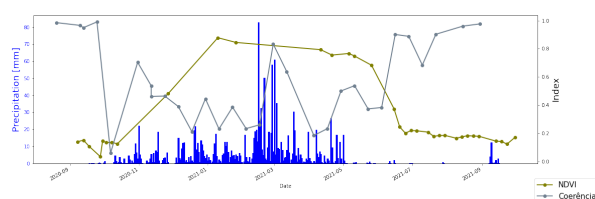


Figure 3: NDVI, Coherence, and Precipitation

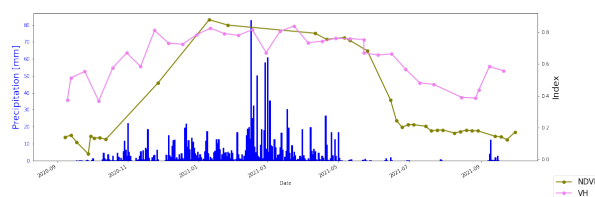


Figure 4: NDVI, VH Backscatter, and Precipitation

Then, according to the data presented in the Tables 1 and 2 with the NDVI and Precipitation intervals, NDVI is below 0.50, the mean and median differences between NDVI and backscatter (both VH and VV) are greater, but

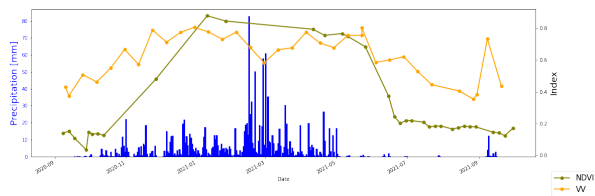


Figure 5: NDVI, VV Backscatter, and Precipitation

are reduced as NDVI increases. However, such values do not vary proportionally to precipitation, even when it reaches values greater than 20 mm. There is no proportional, or even expressive, change in any NDVI interval. This result goes according to the one proposed by [17] which verified a significant difference in backscattering in exposed soil areas, but not as significant in vegetated areas.

NDVI	Average NDVI - VH	Median NDVI - VH	Average NDVI - VV	Median NDVI - VV	Precipitation
<50	-0.2379	-0.2429	-0.1992	-0.1983	<1
<50	-0.4377	-0.4336	-0.4129	-0.4074	1-5
<50	-0.4261	-0.4359	-0.4146	-0.4309	5-10
<50	-0.5424	-0.5484	-0.5315	-0.5358	10-20
<50	-0.3657	-0.3668	-0.3052	-0.2844	20-30
50-75	-0.0852	-0.0882	-0.0454	-0.0468	<1
50-75	-0.1427	-0.1515	-0.1004	-0.0983	1-5
50-75	-0.1272	-0.1312	-0.0853	-0.0896	5-10
50-75	-0.1992	-0.2317	-0.1426	-0.1760	10-20
50-75	-0.1578	-0.1593	-0.0885	-0.0962	20-30
>75	0.0295	0.0109	0.0694	0.0633	<1
>75	0.0889	0.0611	0.0762	0.0739	1-5
>75	0.0850	0.0854	0.1395	0.1464	5-10
>75	-	-	-	-	10-20
>75	0.0050	-0.0097	0.0627	0.0616	20-30

Table 1: NDVI difference values and VH, VV bands, grouped by precipitation and NDVI.

NDVI	Average NDVI - corr	Median NDVI - corr	Precipitation
<50	-0.5391	-0.6384	<1
<50	-0.0343	0.0340	1-5
<50	-0.3116	-0.3604	5-10
<50	-0.0521	-0.0260	10-20
<50	-0.0604	-0.0821	20-30
50-75	0.2332	0.2599	<1
50-75	0.3591	0.3750	1-5
50-75	0.3301	0.3662	5-10
50-75	0.3762	0.3898	10-20
50-75	0.2198	0.2927	20-30
>75	0.5048	0.5216	<1
>75	0.5438	0.5646	1-5
>75	0.3521	0.3347	5-10
>75	-	-	10-20
>75	0.3766	0.4941	20-30

Table 2: NDVI difference values with coherence band, grouped by precipitation and NDVI.

Figures 6 and 7 obtained from the classification allowed us to visualize the distribution of training points in the study area. In these figures it is possible to see the behavior when we removed the images with precipitation in the previous 24 hours, that have a more significant presence of the pasture class.

	Native	Pasture	Double Crop
Native	44	2	0
Pasture	2	31	3
Double Crop	1	2	87

Table 3: Confusion matrix with all crop year data

	Native	Pasture	Double Crop
Native	38	1	0
Pasture	3	15	4
Double Crop	0	12	99

Table 4: Confusion matrix only with products without precipitation in the last 24 hours

	Full	No Precipitation
Accuracy	0,93	0,88
Kappa	0,88	0,78

Table 5: Accuracy and kappa index values



Figure 6: Classification SVM for the study area and location of land use and land cover data collected in the Sinop region, Mato Grosso, Brazil, using all available images.



Figure 7: Classification SVM for the study area and location of land use and land cover data collected in the Sinop region, Mato Grosso, Brazil, using only images without previous precipitation.

4. DISCUSSION

Similarly, about the mean and median differences between NDVI and coherence, there was a progression of negative differences to positive differences during the crop development cycle, however, this variation occurred almost uniformly, regardless of precipitation values. It is noted that, due to the temporal resolution of Sentinel-1, it was not expected that the coherence would present clear variations directly linked to precipitation values, but it could be assumed that with high precipitation values, coherence was unable to detect changes between images, which was not observed.

Therefore, the results demonstrate the non-influence of precipitation on backscatter values for areas with crops. Indicating that the precipitation variable may not be significant as a criterion for removing Sentinel-1 products from a homogeneous dataset, unlike that proposed by [18].

With the accuracy and kappa index of the classification (Table ??), in addition to the confusion matrices (Table 3 and Table 5), the best case scenario is the one that uses all images of the period. This remains contrary to that proposed by [18], concerning the use of precipitation as a criterion for the removal or not of Sentinel 1 products.

However, it is worth noting that the spatial resolution of the meteorological data, of 200 meters, may have influenced the results since the precipitation data were the same for the entire study area. This fact may have been crucial so that precipitation did not appear to be a criterion for the removal or not of Sentinel-1 products.

5. CONCLUSIONS

In this work, we verified the degree of impact of precipitation on the backscatter coefficient of SAR images. In any polarization and also on coherence products, there was a clear impact on signal values in agricultural crop areas.

Moreover, after performing a supervised classification with and without the removal of data in the occurrence of precipitation in the 24 hours before the passage of Sentinel 1, there was no advantage in removing the dates with precipitation in the 24 hours before the passage of the satellite. Also, it was possible to notice that both accuracy and kappa index had worse performance when the classification was made by removing products with possible interference of precipitation the previous 24 hours. Thus, at first, it is suggested that such products should not be removed from the database when precipitation occurs.

As further steps we suggest that this analysis be repeated using local meteorological stations, aiming to increase the precision of the results. Also, it suggested that the same study be repeated using other SAR products, to evaluate possible impacts in different wavelengths.

6. REFERENCES

- [1] Nikos Alexandratos and Jelle Bruinsma. World agriculture towards 2030/2050: the 2012 revision. 2012.
- [2] Steffen Fritz, Linda See, Juan Carlos Laso Bayas, François Waldner, Damien Jacques, Inbal Becker-Reshef, Alyssa Whitcraft, Bettina Baruth, Rogerio Bonifacio, Jim Crutchfield, et al. A comparison of global agricultural monitoring systems and current gaps. *Agricultural systems*, 168:258–272, 2019.
- [3] Zhixin Qi, Anthony Gar-On Yeh, Xia Li, and Zheng Lin. A novel algorithm for land use and land cover classification using radarsat-2 polarimetric sar data. *Remote Sensing of Environment*, 118:21–39, 2012.
- [4] Laura Dingle Robertson, Andrew Davidson, Heather McNairn, Mehdi Hosseini, Scott Mitchell, Diego De Abelleira, Santiago Verón, and Michael H Cosh. Synthetic aperture radar (sar) image processing for operational space-based agriculture mapping. *International Journal of Remote Sensing*, 41(18):7112–7144, 2020.
- [5] G Martis, O Ranta, A Molnar, A Păcurar, et al. Analysis of synthetic aperture radar for agriculture applications: a review. *ProEnvironment*, 12(38):240–245, 2019.
- [6] DE Weissman, G Apgar, JS Tongue, and MA Bourassa. Correcting scatterometer winds by removing rain effects, 2005.
- [7] Clayton Alcarde Alvares, José Luiz Stape, Paulo Cesar Sentelhas, JL de M Gonçalves, Gerd Sparovek, et al. Köppen's climate classification map for brazil. *Meteorologische Zeitschrift*, 22(6):711–728, 2013.
- [8] Africa Ixmuca Flores-Anderson, Kelsey E Herndon, Rajesh Bahadur Thapa, and Emil Cherrington. The sar handbook: Comprehensive methodologies for forest monitoring and biomass estimation. Technical report, 2019.
- [9] Fahim Irshad, Jahanzeb Malik, and Rao Muhammad Zahid Khalil. Mapping wet snow using sar c-band through google earth engine. In *2019 Sixth International Conference on Aerospace Science and Engineering (ICASE)*, pages 1–5. IEEE, 2019.
- [10] Batuhan Osmanoğlu, Filiz Sunar, Shimon Wdowinski, and Enrique Cabral-Cano. Time series analysis of insar data: Methods and trends. *ISPRS Journal of Photogrammetry and Remote Sensing*, 115:90–102, 2016.
- [11] Jiali Shang, Jianguo Liu, Valentin Poncos, Xiaoyuan Geng, Budong Qian, Qihao Chen, Taifeng Dong, Dan Macdonald, Tim Martin, John Kovacs, et al. Detection of crop seeding and harvest through analysis of time-series sentinel-1 interferometric sar data. *Remote Sensing*, 12(10):1551, 2020.
- [12] Thomas Andrew Logan and Jeremy B Nicoll. Automated rtc and insar stack-processing at the alaska satellite facility. In *AGU Fall Meeting Abstracts*, volume 2018, pages G41B–0686, 2018.
- [13] JW Rouse Jr, RH Haas, JA Schell, and DW Deering. Paper a 20. In *Third Earth Resources Technology Satellite-1 Symposium: The Proceedings of a Symposium Held by Goddard Space Flight Center at Washington, DC on*, volume 351, page 309, 1973.
- [14] Onesimo Mutanga and Lalit Kumar. Google earth engine applications, 2019.
- [15] Noel Gorelick, Matt Hancher, Mike Dixon, Simon Ilyushchenko, David Thau, and Rebecca Moore. Google earth engine: Planetary-scale geospatial analysis for everyone. *Remote sensing of Environment*, 202:18–27, 2017.
- [16] Vladimir Vapnik. *The nature of statistical learning theory*. Springer science & business media, 1999.
- [17] Giuseppe Satalino, Anna Balenzano, Francesco Mattia, and Malcolm WJ Davidson. C-band sar data for mapping crops dominated by surface or volume scattering. *IEEE Geoscience and Remote Sensing Letters*, 11(2):384–388, 2013.
- [18] Mohammad El Hajj, Nicolas Baghdadi, Mehrez Zribi, and Sebastien Angelliaume. Analysis of sentinel-1 radiometric stability and quality for land surface applications. *Remote Sensing*, 8(5):406, 2016.